

Complexity Bounds on Quantum Search Algorithms in finite-dimensional Networks

Stefan Boettcher^{1,*}, Shanshan Li¹, Tharso D. Fernandes^{2,3}, and Renato Portugal²

¹*Department of Physics, Emory University, Atlanta, GA 30322; USA*

²*Laboratório Nacional de Computação Científica, Petrópolis, RJ 25651-075; Brazil*

³*Universidade Federal do Espírito Santo, Alegre, ES 29500-000; Brazil*

We establish a lower bound concerning the computational complexity of Grover’s algorithms on fractal networks. This bound provides general predictions for the quantum advantage gained for searching unstructured lists. It yields a fundamental criterion, derived from quantum transport properties, for the improvement a quantum search algorithm achieves over the corresponding classical search in a network based solely on its spectral dimension, d_s . Our analysis employs recent advances in the interpretation of the venerable real-space renormalization group (RG) as applied to quantum walks. It clarifies the competition between Grover’s abstract algorithm, i.e., a rotation in Hilbert space, and quantum transport in an actual geometry. The latter is characterized in terms of the quantum walk dimension d_w^Q and the spatial (fractal) dimension d_f that is summarized simply by the spectral dimension of the network. The analysis simultaneously determines the optimal time for a quantum measurement and the probability for successfully pin-pointing a marked element in the network. The RG further encompasses an optimization scheme devised by Tulsi that allows to tune this probability to certainty, leaving quantum transport as the only limiting process. It considers entire families of problems to be studied, thereby establishing large universality classes for quantum search, which we verify with extensive simulations. The methods we develop could point the way towards systematic studies of universality classes in computational complexity to enable modification and control of search behavior.

I. INTRODUCTION

Quantum walk present one of the frameworks in which quantum computing can satisfy its promise to provide a speed-up over classical computation. It applies to a significant number of interesting problems such as quantum search [1, 2], element distinctness [3, 4], graph isomorphisms [5–7], and circuit design [8]. Analog to random walks, which have been of fundamental importance for the development of stochastic algorithms in classical computing [9, 10], quantum walks have been established as a universal model of quantum computing [11–13]. Similarly, the *physical* properties of quantum walks in localization [14–16], in entanglement [17–19], in in-

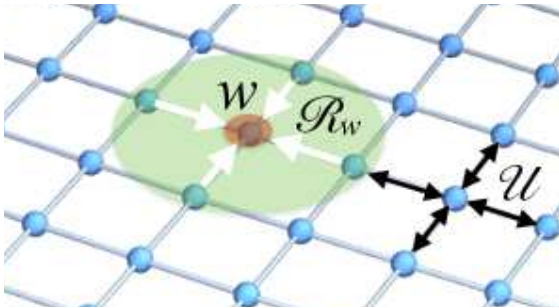


Figure 1. In Grover’s quantum search algorithm, the search-operator \mathcal{R}_w affects an accumulation (white arrows) of the wave-function $\psi_{x,t}$ onto the marked site, w , but only from its neighborhood (shaded). The walk-operator \mathcal{U} transports ψ uniformly between mutually linked sites (black arrows), replenishing neighbors of w in the process. This distinction only arises in a finite-dimensional geometry; it is moot in Grover’s original work [1], where all N sites are linked.

terference [20], in decoherence [21], in topological invariants [22], etc [23], rival classical diffusion as an important transport problem [24–26]. In fact, numerous experimental realizations of quantum walks have been proposed and studied in waveguides [27], in photonics [8, 15, 19, 28], and in atomic physics [29–32]. Photosynthesis provides even a natural occurrence [33, 34].

Grover [1] has developed a quantum algorithm that, starting from an initial state of uniform weight, can locate an entry in an unordered database of N elements with high probability in a time that scales as $\sim \sqrt{N}$. This presents a quadratic speed-up over classical search algorithms and has inspired countless algorithmic developments [35–42] and recently several physical implementations [29, 43, 44]. In a database with a non-trivial network geometry, as in Fig. 1, what we shall call a *spatial* Grover search is faced with the competition between

- (1) the accumulation of weight on a marked entry (or “site”) w at the expense of its neighbors and
- (2) the ability to transport weight via quantum walk into that neighborhood.

Here we show how both of these tasks simultaneously can be described (and optimized) with the real-space renormalization group (RG) [45]. As a result, see Fig. 2, we infer a lower bound on the complexity (or asymptotic computational cost) of spatial Grover search in terms of the network’s fractal dimension d_f and quantum walk dimension d_w^Q or, alternatively, it’s spectral dimension d_s . To this end, we study the exact RG on several fractal networks exemplified by the dual Sierpinski gasket here; the corresponding calculation for the other networks in Fig. 2 follows from their RG in Refs. [46, 47]. Each

of these networks obtains the foregoing results in a non-trivial (and often distinct [47]) manner, which suggests (but does not prove) that our prediction for the complexity bound exhibited in Fig. 2 holds for networks of finite d_s generally. And although we assail fundamental tenets of computer science by exploring the Grover algorithm where it *fails* to saturate its optimal limit, it is exactly in this regime, $1 < d_s < 2$, where we gain the necessary insight to understand its behavior for all dimensions.

A discrete-time quantum walk with a coin was instrumental in the earliest implementations of a quantum search algorithm to reach the Grover limit ($\sim \sqrt{N}$) in as low as two dimensions [40, 48], up to logarithmic corrections, although alternative implementations have been found [36, 39, 49]. While the accumulation in (1) inherently [50] requires at least $\sim \sqrt{N}$ updates, in (2) the neighborhood is replenished by quantum transport on a time-scale of $\sim N^{d_w^Q/d_f}$, as we will show. It becomes the limiting cost for the entire search when $d_f < 2d_w^Q$. The walk dimension $d_w (= d_w^R)$ has been introduced for random walks as the exponent that characterizes the asymptotic scaling relation between the spatial and temporal extend in the probability density function [26, 51], $\rho(x, t) \sim f(|x|^{d_w}/t)$. Such a scaling is a powerful notion that in statistical physics has led to the invention of the Nobel prize winning idea of the renormalization group (RG) [52, 53], as discussed in many textbooks [45]. We shall assume that such a scaling, now with some $d_w = d_w^Q$, also exists for a the quantum walk with wave function $\psi_{x,t}$, where $\rho(x, t) = |\psi_{x,t}^2|$. On a line, so-called weak-limit results [54] verify scaling with $d_w^Q = 1$, which has been reproduced with RG [55]. This result, $d_w^Q = 1$, has been extended to regular lattices in all dimensions [56]. The networks we consider usually lack the translational invariance essential to prove properties on lattice where $d_f = d$ is integer. Yet, our generalized results for real (fractal) dimensions incorporate those for regular lattices. They show that the Grover-limit can always be achieved in dimensions $d > 2$, where the average distance between sites on those lattices is $\sim N^{d_w^Q/d} \ll \sqrt{N}$, and in the critical dimension $d = 2$ with likely logarithmic corrections. In turn, in the mean-field limit [45], when all sites are neighbors (complete graph), it is $d_f = \infty$ and transport is instantaneous, as it is for random graphs of finite degree [41] with typical distances that are $\sim \ln N$.

The naive application of Grover's algorithm on a finite-dimensional geometry also impacts the probability $p = |\psi_{w,t_{\text{opt}}}^2|$ to overlap with the marked site w – the objective of the search – when the measurement is undertaken at the optimal time t_{opt} . The RG we discuss below finds asymptotically for large N that $t_{\text{opt}} \sim N^{d_w^Q/d_f}$, accompanied by a decrease of $p \sim N^{1-2d_w^Q/d_f}$ when $2d_w^Q/d_f > 1$, which is comparable to the optimal overlap with the target element found in a continuous-time quantum walk [42, 59]. Thus, the complexity $c(N)$ of this naive quantum search algorithm, which is given by

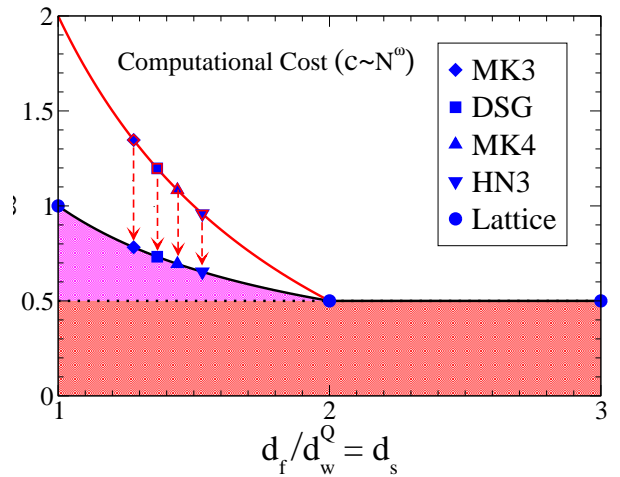


Figure 2. Illustration of the computational cost $c \sim N^\omega$ as a function of d_f/d_w^Q . The systems studied with RG all possess $d_f/d_w^Q < 2$, where the Grover limit ($\omega = \frac{1}{2}$) can not be reached and the scaling is non-trivial. The naive Grover search algorithm, analyzed in Sec. III, achieves the scaling in Eq. (1) (red line, red-framed symbols), which can be optimized (down-arrows) by Tulsi's method [57], see Eq. (2) (black line, blue symbols). Aside from log-corrections, the RG finds $\omega = \max\left\{\frac{d_w^Q}{d_f}, \frac{1}{2}\right\}$, which provides a fundamental limit, constraint by quantum transport through the network geometry for $d_f/d_w^Q < 2$ (magenta-shaded area) or else by the inherent Grover limit of rotating the state vector in Hilbert space [50] (red-shaded area). Assuming $d_w^Q = \frac{1}{2}d_w^R$, as obtained in Ref. [47], all results can be expressed purely via the spectral dimension of the network Laplacian, for which it is known that $d_s = 2d_f/d_w^R$ [58]. We treat DSG as example here; the values for d_f/d_w^Q listed here for other networks – MK3, MK4, and HN3, i.e., 3 and 4-regular Migdal-Kadanoff and Hanoi networks – are adapted from Tab. 1 in Ref. [46]. Since $d_w^Q = 1$ on a d -dimensional lattice, i.e., $d_s = d_f = d$, this diagram applies directly to lattices, with $d = 2$ as the critical dimension [45].

the product of t_{opt} with the necessary number of repeat-measurements ($\sim 1/p$), becomes

$$c = \frac{t_{\text{opt}}}{p} \sim \max\left\{\sqrt{N}, N^3 \frac{d_w^Q}{d_f} - 1\right\}. \quad (1)$$

We have verified the RG-predictions for both, t_{opt} and p , for several other networks, see Fig. 2, and with numerical simulations, explained in Fig. 5. Furthermore, an optimized algorithm was developed by Tulsi [57] that we can directly analyze with RG also. It allows to boost the overlap p at the expense of at most two extra qubits, when the eigenvalue with the smallest positive argument of the evolution operator fulfills certain properties. Then, the overlap always can be tuned to a finite value, $p \sim 1$, independent of N , and the complexity bound finally attains its optimal form

$$c_{\text{Tulsi}} \sim \max\left\{\sqrt{N}, N^3 \frac{d_w^Q}{d_f}\right\}. \quad (2)$$

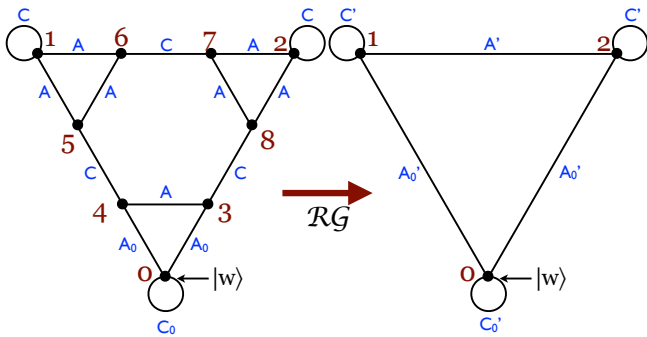


Figure 3. Depiction of the (final) RG-step in the analysis of DSG. Recursively, the inner-6 sites (here labeled 3, . . . , 8) of each larger triangle (left) in DSG are decimated to obtain a reduced triangle (right) with renormalized hopping operators (primed). Since site $w = 0$ is distinct, modified recursion rules apply for the matrices labeled with subscript 0.

The dependence of the scaling of c with N on d_f/d_w^Q for both of these scenarios is illustrated in Fig. 2. Ultimately, our RG calculation below implies that the algorithmic complexity is constrained by the speed of quantum transport: If $d_f/d_w^Q > 2$, Grover’s limit can be reached!

For coined quantum walks with no marked nodes it has been shown previously that there is a relation between quantum walks and the corresponding classical random walk [46, 47], i.e., $d_w^Q = \frac{1}{2}d_w^R$. Using $d_w^R/d_f = 2/d_s$ [58], we can represent Eqs. (1-2) purely in spectral terms, i.e., $d_f/d_w^Q = d_s$, as indicated in Fig. 2. In that case, our result mirrors Szeged’s finding for “hitting times” of $1/\sqrt{\delta} \sim N^{\frac{1}{d_s}}$ in bipartite networks with spectral gap δ in quantized Markov chains [60, 61]. A similar result has also been shown for quantum first passage times [62].

II. METHODS

1. Quantum Evolution Equation

The time evolution of a quantum walk is governed by the discrete-time equation

$$|\Psi_{t+1}\rangle = \mathcal{U}|\Psi_t\rangle \quad (3)$$

with unitary propagator \mathcal{U} . It resembles closely the master equation for a random walk (or any other Markov process), for which \mathcal{U} would be a stochastic operator. Then, in the discrete N -dimensional site-basis $|x\rangle$ with $\psi_{x,t} = \langle x|\Psi_t\rangle$, the probability density function is given by $\rho(x,t) = |\psi_{x,t}|^2$. In this basis, the propagator can be represented as an $N \times N$ matrix $U_{x,y} = \langle x|\mathcal{U}|y\rangle$ with operator-valued entries that describe the transitions between neighboring sites (“hopping operators”). To study the long-time dynamics, it is advantageous to apply a discrete Laplace transform [26],

$$\bar{\psi}_x(z) = \sum_{t=0}^{\infty} \psi_{x,t} z^t, \quad (4)$$

such that Eq. (3) becomes

$$\bar{\psi}_x = \sum_y z U_{x,y} \bar{\psi}_y + \psi_{x,t=0}. \quad (5)$$

The self-similarity of fractal networks allows for a decomposition of $U_{x,y}$ into its smallest sub-structures, exemplified by Fig. 3. It shows the elementary graph-let of nine sites that is used to recursively construct the dual Sierpinski gasket (DSG). The master equations pertaining to these sites are:

$$\begin{aligned} \bar{\psi}_0 &= (M_0 + C_0) \bar{\psi}_0 + A(\bar{\psi}_3 + \bar{\psi}_4) + I_0 \psi_{IC}, \quad (6) \\ \bar{\psi}_{\{1,2\}} &= (M + C) \bar{\psi}_{\{1,2\}} + A(\bar{\psi}_{\{5,7\}} + \bar{\psi}_{\{6,8\}}) + I \psi_{IC}, \\ \bar{\psi}_{\{3,4\}} &= M \bar{\psi}_{\{3,4\}} + C \bar{\psi}_{\{8,5\}} + A_0 \bar{\psi}_0 + A \bar{\psi}_{\{4,3\}} + I \psi_{IC}, \\ \bar{\psi}_{\{5,6,7,8\}} &= M \bar{\psi}_{\{5,6,7,8\}} + C \bar{\psi}_{\{4,7,6,3\}} \\ &\quad + A(\bar{\psi}_{\{1,5,2,7\}} + \bar{\psi}_{\{6,1,8,2\}}) + I \psi_{IC}. \end{aligned}$$

The hopping operators A and C describe transitions between neighboring sites, while M (not shown in Fig. 3) permits the walker to remain on its site in a “lazy” walk. The inhomogeneous ψ_{IC} -terms allow for an initial condition $\psi_{x,t=0}$ on the respective site x .

Preserving the norm of the quantum walk demands unitary propagation, i.e., $\mathbb{I} = \mathcal{U}^\dagger \mathcal{U}$. This can be achieved in the discrete-time case only when the hopping operators like $\{A, C, M\}$ in Eqs. (6) are matrices, not scalars. Correspondingly, the state of the walk at each site, $\psi_{x,t}$, must be a vector of conforming length. Each update, a conforming coin matrix C entangles the components of the state vector, which the hopping operators subsequently distribute to their respective neighboring site. For coined quantum walks, it has been conventional to consider merely those coins whose dimensions adhere to the degree of the sites in the network under investigation. Then, each component of a site’s state vector is shifted along one specific direction at each update, ensuring the unitarity of the propagator \mathcal{U} overall. However, for networks of higher degree, or of mixed degree, this approach becomes quite unwieldy, if not impossible. In Appendix A, we have laid out how to obtain generalized unitarity conditions for any network. When applied to DSG specifically, we have derived the following conditions concerning the hopping operators in Eqs. (6):

$$\begin{aligned} \mathbb{I} &= A^\dagger A + B^\dagger B + C^\dagger C + M^\dagger M, \quad (7) \\ 0 &= A^\dagger B + B^\dagger M + M^\dagger A = C^\dagger M + M^\dagger C = A^\dagger C = B^\dagger C. \end{aligned}$$

These conditions at hand, we can now systematically design generalized hopping operators $\{A, B, C, M\}$. We make a most simple choice by requiring an additional symmetry, $A = B$, while choosing 2×2 -matrices

$$M = \begin{bmatrix} -\frac{1}{3} & 0 \\ 0 & 0 \end{bmatrix} C, \quad A = \begin{bmatrix} \frac{2}{3} & 0 \\ 0 & 0 \end{bmatrix} C, \quad C = \begin{bmatrix} 0 & 0 \\ 0 & 1 \end{bmatrix} C, \quad (8)$$

that satisfy Eqs. (7) for any unitary coin \mathcal{C} . Here, the most general unitary 2×2 coin matrix is given by

$$\mathcal{C} = \begin{pmatrix} \sin \eta & e^{i\chi} \cos \eta \\ e^{i\vartheta} \cos \eta & -e^{i(\chi+\vartheta)} \sin \eta \end{pmatrix}. \quad (9)$$

In the following, we merely consider variable η but set $\chi = \vartheta = 0$. [We note that for non-zero χ and ϑ , the following results would be identical aside from a trivial rotation in the Laplace parameter, $z \rightarrow z e^{-i(\chi+\vartheta)}$.] However, with the free parameter η , which specifies the extent by which the components of the state vector get entangled, we are now in a position to study an entire family of problems. Even though the degree of the network is larger than this coin-space, for the Hadamard coin in Eq. (9) we show in the following that it reproduces the phenomenology of the quantum walk with 3×3 -matrices and lower symmetry ($A \neq B$) for the Grover coin described in Refs. [47, 63]. Besides this “minimalist” example, other interesting 3 (or higher) dimensional matrices that solve the conditions in Eq. (7) may exist, potentially harboring new universality classes and localization behaviors [64].

In Eqs. (6), we have distinguished site $w = 0$. (This choice is largely a matter of convenience; any other w would result in the same scaling but with a w -dependent pre-factor [65].) In such a way, we can study either a quantum walk starting on that site to determine the spreading dynamics or the quantum search problem of amplifying the wave-function on site $w = 0$ after starting from a uniform initial state $\psi_{x,0} = \frac{1}{\sqrt{N}} \psi_{IC}$, where ψ_{IC} denotes an initial state-vector. The latter case is discussed below. In the former case, the initial condition is localized at w , $\psi_{x,t=0} = \delta_{x,w} \psi_{IC}$, with $I_0 = \mathbb{I}$, $I \equiv 0$, $M_0 = M$, $A_0 = A$, and $C_0 = C$, as discussed elsewhere [47]. Although they result in very different physical situations, both cases built on the following analysis of the RG-recursions for the homogeneous walk, irrespective of the initial conditions I .

2. RG for the Homogeneous Quantum Walk

As we have indicated in the introduction, the real-space RG for a walk [26] provides information that relates the temporal and spatial spreading of the walk. Instead of yielding a specific, quantitative result on a question of, say, “How much time T , on average, does it take for a walk to fall off a table of base-length L after starting in its center?”, the RG answers the *scaling* question “By how much does a change in $L_k \rightarrow L_{k+1} = 2L_k$ rescale time $T_k \rightarrow T_{k+1} = \lambda T_k$?” in each step $k \rightarrow k+1$ of the RG. Assuming scaling $T_k \sim L_k^{d_w}$ (at least asymptotically for all large k), the answer to that question would imply $d_w = \log_2 \lambda$. Clearly, for a classical random walk (i.e., diffusion) on any d -dimensional “table” it is $\lambda = 4$, i.e., $d_w = 2$. In a fractal geometry, the answer to this question generally is non-trivial [26, 51]. This example illustrates the relevance of RG for the complexity of the Grover algorithm which concerns the question on “How much does

t_{opt} for search increase when I increase $N (= L^{d_f})$ ”. Note, however, that due to the Laplace transform in Eq. (4) the large- t limit is accessed for $z \rightarrow 1$ here.

The recursive structure of DSG (and many other fractals, such as those discussed in Ref. [46]), allows to establish exact recursion relations between a walk at length k and $k+1$. These RG-recursions for the DSG, as represented by Eqs. (44), are generic and have been derived previously [47]. In Appendix B, we recall how to obtain those recursions, for completeness. Iterating these RG-recursions as described there for only one step already reveals a recursive pattern that suggests the parametrization

$$\begin{aligned} M_k &= \left(a_k - \frac{2}{3} b_k \right) \begin{bmatrix} 1 & 0 \\ 0 & 0 \end{bmatrix} \mathcal{C}, \\ A_k &= \left(a_k + \frac{1}{3} b_k \right) \begin{bmatrix} 1 & 0 \\ 0 & 0 \end{bmatrix} \mathcal{C}, \\ C_k &= z \begin{bmatrix} 0 & 0 \\ 0 & 1 \end{bmatrix} \mathcal{C}, \end{aligned} \quad (10)$$

which *exactly* closes on itself after one iteration, $k \rightarrow k+1$, when we identify for the *scalar* RG-flow:

$$\begin{aligned} a_{k+1} &= \frac{(9a_k b_k + 3z a_k - 2z b_k) \sin \eta}{3(3z - 6a_k + b_k) \sin \eta + 3(3 - 6z a_k + z b_k)}, \\ b_{k+1} &= \frac{2(9a_k b_k^2 + 3z a_k b_k + z b_k^2 - 3z^2 a_k + 2z^2 b_k) \sin^2 \eta + 4(1 - z^2)(6a_k b_k - b_k^2) \sin \eta + 2(3a_k - 2b_k - 3z a_k b_k - z b_k^2 - 9z^2 a_k b_k^2)}{2(6a_k b_k - b_k^2 + 3z a_k + z b_k + 3z^2) \sin^2 \eta + 4(1 - z^2)(3a_k - 2b_k) \sin \eta - 2(3 + 3z a_k + z b_k + 6z^2 a_k b_k - z^2 b_k^2)}. \end{aligned} \quad (11)$$

This flow is initiated at $k = 0$ with $a_{k=0} = z/3$ and $b_{k=0} = z$, to match Eqs. (10) to the unrenormalized hopping operators in Eqs. (8). Note that these RG-flow recursions are vastly simpler than the 5-term recursions previously reported in Ref. [63], or those in Ref. [47], even though here they describe an entire family of coins via the coin-parameter η .

As explained above, the real-space RG equations encapsulate the behavior of the physical process under rescaling of length (on DSG, from base-length $L_k = 2^k$ to $L_{k+1} = 2L_k$, while size $N_k = L_k^{d_f} = 3^k$ changes by a factor of 3, i.e., $d_f = \log_2 3$). Thus, we now proceed to study the fixed-point properties of the RG-flow in Eq. (11) at $k \sim k+1 \rightarrow \infty$ near $z \rightarrow 1$ [26]. The particular combination of a_k and b_k in Eq. (10) ensures that the Jacobian of the fixed point already is diagonal, with eigenvalues $\lambda_1 = 3$ and $\lambda_2 = \frac{5}{3}$. Extending the expansion of Eq. (11) in powers of $\zeta = z - 1$ for $k \rightarrow \infty$ to sufficiently-high order, we obtain:

$$\begin{aligned} a_k(z) &\sim \frac{1}{3} + \zeta \mathcal{A} \lambda_1^k + \zeta^2 \alpha_k^{(2)} + \zeta^3 \alpha_k^{(3)} + \dots, \\ b_k(z) &\sim 1 + \zeta \mathcal{B} \lambda_2^k + \dots, \end{aligned} \quad (12)$$

with unknown constants \mathcal{A} and \mathcal{B} . Here, we defined

$$\begin{aligned}\alpha_k^{(2)} &\sim \frac{3}{2}\mathcal{A}^2\lambda_1^{2k} + \dots, \\ \alpha_k^{(3)} &\sim \frac{9}{4}\mathcal{A}^3\lambda_1^{3k} - \frac{3}{8}\mathcal{A}^2\mathcal{B}\lambda_1^{2k}\lambda_2^k + \dots,\end{aligned}\quad (13)$$

where we have only kept leading-order terms relevant for the following considerations. It was argued previously [47, 66] that we can identify:

$$d_f = \log_2 \lambda_1, \quad d_w^Q = \log_2 \sqrt{\lambda_1 \lambda_2}, \quad (14)$$

i.e., $d_f = \log_2 3$ and $d_w^Q = \log_2 \sqrt{5}$ for DSG.

III. RESULTS FOR THE COMPLEXITY OF QUANTUM SEARCH

To apply the RG results in Sec. II to the corresponding quantum search problem, we use the *abstract search algorithm* [1, 40, 48]. It replaces the operator \mathcal{U} by an equally unitary “search”-propagator $\mathcal{U}_w = \mathcal{U} \cdot \mathcal{R}_w$ that distinguishes the sought-after site $|w\rangle$ from the remaining sites using the search-operator

$$\mathcal{R}_w = \mathbb{I} - |w\rangle\langle w| (2D). \quad (15)$$

The walk operator \mathcal{U} corresponds to the inversion-about-average operator defined by Grover [1]. It “drives” the quantum walk by transporting the weight of the wave-function between neighboring sites in an attempt to make it uniform. Alas, in the quantum search, which starts from a uniform state, the prior reflection of the phase at site w by \mathcal{R}_w first imbalances the amplitude there, before \mathcal{U} now amplifies this imbalance at w . Thus, site w acts as an “attractor” for the weight of the wave-function at the expense of its immediate neighbors - a deficit that \mathcal{U} persistently tries to correct. Since we require \mathcal{U}_w to be unitary, so must be \mathcal{R}_w in Eq. (15), which implies the condition

$$2D^\dagger D = D^\dagger + D. \quad (16)$$

Grover [1], and by default many authors since, have further imposed reflectivity, $\mathcal{R}_w^2 = \mathbb{I}$, which conveniently reduces Eq. (16) to $D = D^2$, further implying hermiticity, $D = D^\dagger$. These conditions on D still allow for entire classes of operators, as well as $D = \mathbb{I}$. We will consider first the family,

$$D(\gamma) = \begin{bmatrix} \cos^2 \gamma & \sin \gamma \cos \gamma \\ \sin \gamma \cos \gamma & \sin^2 \gamma \end{bmatrix}, \quad (17)$$

which for $\gamma = \frac{\pi}{4}$ reduces to the Grover operator that is widely used in numerical simulations for this task [48]. Note that D in Eq. (17) is singular, $\det D = 0$, for all γ , while $D = \mathbb{I}$ is the unique non-singular solution of $D = D^2$. The RG reveals that $D = \mathbb{I}$ does not allow for an efficient search, as we will show in Sec. III C. Similarly, the RG calculation in Sec. III D implies that reflectivity appears to be necessary condition.

A. General Considerations for Quantum Search on DSG

Uniform initial conditions are provided by $|\Psi_{t=0}\rangle = \frac{1}{\sqrt{N}} \sum_x |x\rangle \otimes |\psi_{IC}\rangle$, i.e., $\psi_{x,t=0} = \frac{1}{\sqrt{N}} \psi_{IC}$. With the goal to optimize the amplitude $\psi_{0,t}$ to detect the walk on the sought-after site $w = 0$ in the shortest time possible, Eq. (5) then becomes

$$\begin{aligned}\bar{\psi}_x &= \sum_y z(\mathcal{U}_w)_{x,y} \bar{\psi}_y + \frac{\psi_{IC}}{\sqrt{N}}, \\ &= \sum_y z\mathcal{U}_{x,y} (\mathbb{I} - 2D\delta_{y,0}) \bar{\psi}_y + \frac{\psi_{IC}}{\sqrt{N}},\end{aligned}\quad (18)$$

which turns into Eqs. (6) when applied to the DSG with $\mathcal{O}_0 = \mathcal{O}(\mathbb{I} - 2D)$ for each $\mathcal{O} \in \{A, C, M, I\}$. After k iterations, in the final step, as shown in Fig. 3, the DSG reduces to a triangle of sites with:

$$\begin{aligned}\bar{\psi}_0 &= (M_k + C_k) (\mathbb{I} - 2D) \bar{\psi}_0 + A_k (\bar{\psi}_1 + \bar{\psi}_2) \\ &\quad + I_k (\mathbb{I} - 2D) \frac{\psi_{IC}}{\sqrt{N}}, \\ \bar{\psi}_{\{1,2\}} &= (M_k + C_k) \bar{\psi}_{\{1,2\}} + A_k \left[(\mathbb{I} - 2D) \bar{\psi}_0 + \bar{\psi}_{\{2,1\}} \right] \\ &\quad + I_k \frac{\psi_{IC}}{\sqrt{N}}.\end{aligned}\quad (19)$$

Solving for $\bar{\psi}_0$, we obtain

$$\bar{\psi}_0 = [\mathbb{I} - (M_k + C_k + V_k A_k) (\mathbb{I} - 2D)]^{-1} (\mathbb{I} + V_k) I_k \frac{\psi_{IC}}{\sqrt{N}} \quad (20)$$

where we abbreviated $V_k = 2A_k (\mathbb{I} - A_k - C_k - M_k)^{-1}$. Note that $\bar{\psi}_0$ appears to depend also on the RG-recursion for I_k . Yet, we can eliminate it by the following consideration: If it were $D = 0$, then we would have $\mathcal{R}_w = \mathbb{I}$ and $\mathcal{U}_w \equiv \mathcal{U}$ for the propagator, which would leave the uniform initial state *invariant*. Thus, $\bar{\psi}_0(z)|_{D=0} = F(z) \frac{\psi_{IC}}{\sqrt{N}}$, where $F(z)$ has at most N -independent, trivial poles. In fact, we find from Eq. (20) at $D = 0$ that

$$\begin{aligned}F(z) &= [\mathbb{I} - (M_k + C_k + V_k A_k)]^{-1} (\mathbb{I} + V_k) I_k, \\ &= \frac{1}{1-z^2} \begin{bmatrix} 1+z \sin \eta & z \cos \eta \\ z \cos \eta & 1-z \sin \eta \end{bmatrix},\end{aligned}\quad (21)$$

independent of k . Then substituting Eq. (21) back into Eq. (20) yields

$$\bar{\psi}_0 = [\mathbb{I} - 2G(z)D]^{-1} F(z) \frac{\psi_{IC}}{\sqrt{N}}, \quad (22)$$

with

$$G(z) = \left[\mathbb{I} - (M_k + C_k + V_k A_k)^{-1} \right]^{-1}. \quad (23)$$

Even before we discuss the effect of the search-operator D , the properties of $G(z)$ itself are crucial for the proper

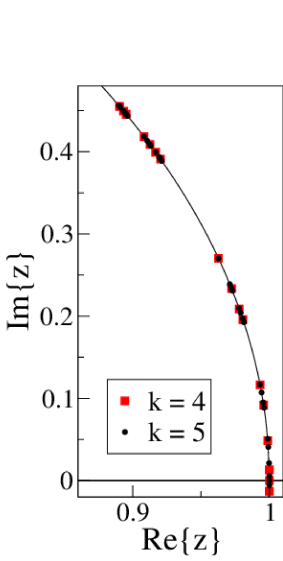


Figure 4. Plot of the poles of the Laplace transform for the amplitude at the sought-for site, $\overline{\psi}_0^{(k)}(z)$ in Eq. (22), in the complex- z plane at RG-steps $k = 4$ (■) and $k = 5$ (●) for quantum search on the dual Sierpinski gasket (DSG). (The poles are certain to occur in complex-conjugate pairs, so only the upper z -plane is shown.) A finite fraction of those poles progressively impinge on the real- z axis at $z = 1$.

interpretation of the quantum search. It closely resembles the Laplace-space amplitude for a quantum walker to remain at its starting location examined previously [47], although that situation has quite different (localized) initial conditions. Inserting the RG-results from Eqs. (10-13) into Eq. (23), we find in powers of $\zeta = z - 1$:

$$G(z) \sim \frac{1}{9\mathcal{A}\lambda_1^k} G_{-1} \zeta^{-1} + G_0 \zeta^0 + \frac{5\mathcal{B}\lambda_2^k}{24} G_1 \zeta^1 + \dots \quad (24)$$

with dominant contributions in large- k from the matrices

$$G_{-1} = \begin{bmatrix} 1 & \frac{\cos \eta}{1 + \sin \eta} \\ \frac{\cos \eta}{1 + \sin \eta} & \frac{1 - \sin \eta}{1 + \sin \eta} \end{bmatrix}, \quad (25)$$

$$G_0 = \frac{1}{2} \begin{bmatrix} 1 & \frac{\cos \eta}{1 + \sin \eta} \\ -\frac{\cos \eta}{1 + \sin \eta} & 1 \end{bmatrix} + \dots,$$

$$G_1 = G_{-1} + \dots$$

The emergence of λ_2^k as the dominant term for large k at order ζ^1 is a consequence of unitarity [47], due to a delicate cancellation between α_2^2 and $(\mathcal{A}\lambda_1^k)\alpha_3$ in Eq. (13). Also, in the following it will prove crucial that G_{-1} in Eq. (25) is a *singular* matrix.

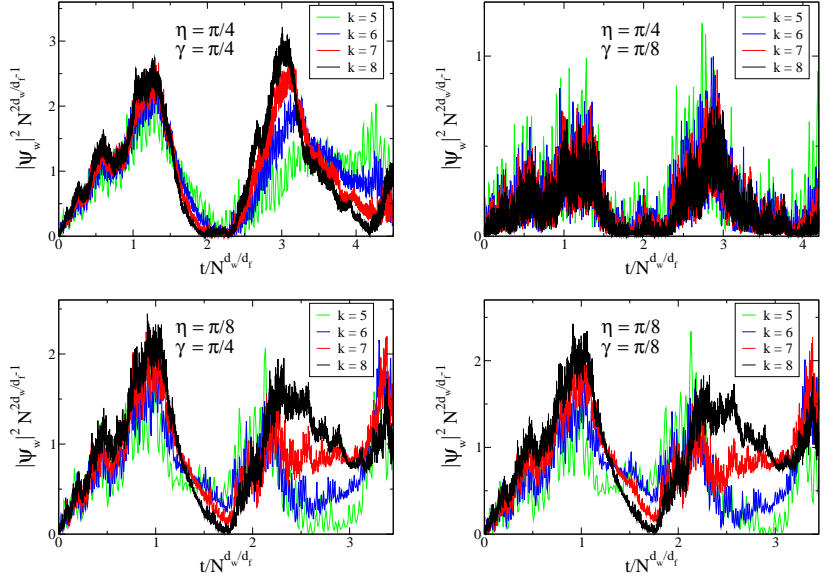


Figure 5. Plot of the probability $p = |\psi_w^2, t|^2$ to detect the quantum walk at site $w = 0$ as a function of time t for all combinations of parameters of the coin in Eq. (9) with $\eta = \pi/4$ and $\pi/8$ and of the search operator in Eq. (17) with $\gamma = \pi/4$ and $\pi/8$ for DSG of size $N_k = 3^k$. (Shown here are $k = 5, \dots, 8$, in order from bottom to top near the first peak at $t/N^{d_w^Q/d_f} \approx 1$.) Appropriately rescaled according to Eq. (30), the data collapses on a quasi-periodic sinusoidal function, as in Eq. (27). For the collapse, we use the value for d_w^Q and d_f according to Eq. (14). The optimal time for a measurement would be at $t_{\text{opt}}/N^{d_w^Q/d_f} \approx 1$, near the first well-formed peak. Smoother (but less insightful) behavior for p would be obtained after implementing Tulsı's method [57] (see also Sec. IIIB1 and the Appendix D) and various improvements of the evolution operator [67, 68].

B. Discussion of D in Eq. (17)

With a search operator containing the generalized Groverian matrix $D(\gamma)$ in Eq. (17), we indeed find a quantum search algorithm with a non-trivial complexity. With $G(z)$ in Eq. (24), we can construct the combination $\mathbb{I} - 2G(z)D$ in Eq. (22), which itself is singular at order ζ^{-1} , due to G_{-1} . It is thus not surprising to find that its inverse in Eq. (22) has a leading contribution of order ζ^0 . The combination of $[\mathbb{I} - 2G(z)D]^{-1}F(z)$ in Eq. (22) should therefore be $\sim \zeta^{-1}$, owing to the pole in $F(z)$. Amazingly, however, the matrix $F(z)$ in Eq. (21) exactly *annihilates* that ζ^{-1} -term in $\overline{\psi}_0$ for any η or γ . Evaluation of Eq. (22) then leads to:

$$\overline{\psi}_0 \sim \left\{ (\mathcal{A}\lambda_1^k) F_0 \zeta^0 + (\mathcal{A}\lambda_1^k)^2 (\mathcal{B}\lambda_2^k) F_2 \zeta^2 + \dots \right\} \frac{\psi_{IC}}{\sqrt{N}} \quad (26)$$

where we have only kept the most-divergent term in k at each order of ζ . Each term contains a k -independent matrix $F_i(\eta, \gamma, \zeta)$ that is regular in ζ and that captures the entire dependence on the coin-parameter η from Eq. (9) and the γ -dependence of the search operator D in Eq. (17). Although each such matrix is singular, every one of their components is a well-behaved function

on $0 < \eta < \frac{\pi}{2}$ and $0 < \gamma < \frac{\pi}{2}$ without poles or selections for which any F_i would vanish entirely. Thus, we can conclude that our following results for the scaling of quantum search are *universal* as far as this choice of coin and search operator is concerned.

To extract the relevant scaling behavior for the amplitude at the sought-for site, $\bar{\psi}_0$ in Eq. (26), we have to discuss the expectation we have for its form [26]. For $t > 0$, $\psi_{0,t}$ should be a periodic function of some fundamental period $T(N) = 2\pi/\theta_k$ that is small at $t = 0$ but rises to a significant maximum with some amplitude-factor $\sim N^\epsilon$ at the optimal time to conduct a measurement, $t_{\text{opt}} = T(N)/4$. Both, the increasing number of Laplace-poles of the RG with increasing system size, shown in Fig. 4, and the additional ‘‘overtones’’ exhibited in the numerical simulations in Fig. 5, would suggest an Ansatz for $\bar{\psi}_0$ as a superposition of modes in a generalized Fourier series, as analyzed in Ref. [47]. However, the discussion in Appendix C confirms that even the simplest Ansatz of considering merely the two closest poles to $z = 1$ suffices here, and we may write

$$\psi_{0,t} \sim N^\epsilon \sin(\theta_k t) \frac{\psi_{IC}}{\sqrt{N}}, \quad (27)$$

which, after Laplace transformation according to Eq. (4), produces two Laplace-poles at $z_0 = e^{\pm i\theta_k}$ symmetrically impinging on $z = 1$ along the unit-circle in the complex- z plane:

$$\begin{aligned} \bar{\psi}_0(z) &\sim \frac{N^\epsilon}{2i} \left(\frac{1}{1 - ze^{i\theta_k}} - \frac{1}{1 - ze^{-i\theta_k}} \right) \frac{\psi_{IC}}{\sqrt{N}}, \\ &\sim N^\epsilon \left[\frac{1}{\theta_k} \zeta^0 - \frac{1}{\theta_k^3} \zeta^2 + \frac{1}{\theta_k^3} \zeta^3 + \frac{1}{\theta_k^5} \zeta^4 + \dots \right] \frac{\psi_{IC}}{\sqrt{N}} \end{aligned} \quad (28)$$

Then, we match Eqs. (26) and (28) term-by-term in ζ to get

$$\frac{N^\epsilon}{\theta_k} \sim \lambda_1^k, \quad \frac{N^\epsilon}{\theta_k^3} \sim \lambda_1^{2k} \lambda_2^k, \quad (29)$$

which provides for the characteristic period and the amplitude at time t_{opt} with $\sin(\theta_k t_{\text{opt}}) = 1$:

$$\begin{aligned} T(N) &\sim \frac{1}{\theta_k} \sim \sqrt{\lambda_1^k \lambda_2^k} \sim N^{\frac{d_w^Q}{d_f}}, \quad (30) \\ |\psi_{0,t}|^2 &\sim \left(\frac{N^\epsilon}{\sqrt{N}} \right)^2 \sim \frac{\lambda_1^k}{N \lambda_2^k} \sim N^{1-2\frac{d_w^Q}{d_f}}, \end{aligned}$$

where we have identified the eigenvalues with the appropriate dimensions as given in Eq. (14). In fact, we have extended the RG-expansion in Eq. (26) to two more orders and found that they scale consistently with the ζ^3 and ζ^4 -terms of Eq. (28). In Figs. 5, we demonstrate that the scaling in Eq. (30) perfectly collapses the data we have obtained from numerical simulations of quantum search on DSG. They yield the computational complexity stated in Eq. (1) and the naive scaling shown in Fig. 2.

In fact, those values for the rescaling of $p = |\psi_{0,t}^2|$ and T in Eq. (30) have been studied numerically before by Patel and Raghunathan [67], who found $p \sim N^{-0.440(4)}$ and $T \sim N^{0.730(2)}$ for a coined quantum search on a regular Sierpinski lattice, which is not too far from the analytical prediction here: $2\frac{d_w^Q}{d_f} - 1 = \log_3 5 - 1 = 0.464974\dots$ and $\frac{d_w^Q}{d_f} = \frac{1}{2} \log_3 5 = 0.732487\dots$. Recently, Tamegai et al [69] found equivalent results also for the Sierpinski carpet (which is not renormalizable). Similarly, Marquezino et al. [68] simulated a quantum search with a modified Grover coin on the Hanoi network (HN3) and found $p \sim N^{-0.37}$ and $T \sim N^{0.65}$, in reasonable agreement with the analytical prediction of $2\frac{d_w^Q}{d_f} - 1 = 0.30576\dots$ and $\frac{d_w^Q}{d_f} = 0.652879\dots$, using $d_w^Q = 2 - \log_2 \frac{\sqrt{5}+1}{2}$ and $d_f = 2$ found for this network [46]. Both of these numerical studies also considered successful implementations of Tulsi’s method to optimize the overlap to become $p \sim 1$, which we explore analytically with the RG in the following.

1. Optimization with Tulsi’s Method:

Tulsi [57] realized that the interplay between walk-operator and search-operator in an implementation of Grover’s algorithm on a low-dimensional geometry can be further optimized by adding at most two ancilla qubits [70]. Thereby, each is doubling the dimensions to the internal coin-space of the quantum walk (which has been compared to giving a Dirac-fermion a position-dependent mass [67]). This minimal extension inserts a tunable parameter τ that allows to ‘‘buffer’’ more weight $|\psi_{0,t}^2|$ only at the sought-after site w in just the right amount so as to optimize $p = |\psi_{0,t}^2|$ to attain a finite, N -independent value just at the time of measurement. The optimal choice for this parameter itself does depend on N but is independent of w . While the implementation details are technical and have been deferred to Appendix D, the calculation follows that in Sec. III A closely but with somewhat enlarged matrices. In the end, we obtain relations almost identical to Eq. (26) but with an overall factor of $\cot \tau$. Then, Eq. (29) generalizes to:

$$\frac{N^\epsilon}{\theta_k} \sim \lambda_1^k \cot \tau, \quad \frac{N^\epsilon}{\theta_k^3} \sim \lambda_1^{2k} \lambda_2^k \cot \tau. \quad (31)$$

Note that the limit $\tau \rightarrow 0$, in which the part of the product-space linked by Tulsi’s ancilla qubits would disconnect, emerges as a singular limit, $\cot \tau \rightarrow \infty$, in the RG. Taking the ratio of both expressions in Eq. (31) cancels the τ -dependence, signifying that the quantum transport scaling expressed by $T \sim 1/\theta_k$ found in Eq. (30) remains unaffected, consistent with the fact that the ancilla merely acts only locally at site w . However, the amplitude at site w , obtained by the product of both relations in Eq. (31) now becomes

$$|\psi_{0,t}|^2 \sim \frac{\lambda_1^k}{N \lambda_2^k} \cot^2 \tau, \quad (32)$$

which in reference to Eq. (30) we are free to optimize via

$$\tau \sim N^{\frac{d_w}{d_f} - \frac{1}{2}} \ll 1, \quad (33)$$

such that $p = |\psi_{0,t}^2| \sim 1$, mindful of the fact that p is bounded by unity, of course. This analytical results reproduces again the numerical predictions and the scaling relations found [67, 68] for Tulsi's parameter τ .

C. Discussion of Search Operator $D = \mathbb{I}$

With the preceding methods, we can also address interesting questions regarding the universality of the results. We have shown that the search operator with the choice of D in Eq. (17) provides a scaling of the complexity that is independent of the parameter γ . In turn, we find that $D = \mathbb{I}$, another choice that satisfies the conditions on the search operator in Eq. (16), will not allow to accumulate weight at the sought-after site w . Following Eq. (25) in Sec. III A, $\mathbb{I} - 2G(z)D$ in Eq. (22) is again singular at order ζ^{-1} , yet, even its inverse in Eq. (22) possesses a leading contribution of order ζ^{-1} and has the expansion:

$$\begin{aligned} [\mathbb{I} - 2G(z)D]^{-1} &\sim -\frac{2}{9(\mathcal{A}\lambda_1^k)}X_{-1}\zeta^{-1} + X_0\zeta^0 \\ &\quad -\frac{5(\mathcal{B}\lambda_2^k)}{12}X_1\zeta^1 + \dots, \end{aligned}$$

with

$$\begin{aligned} X_0 &= \frac{1 + \sin(\eta)}{\cos(\eta)} \begin{bmatrix} 0 & 1 \\ -1 & 0 \end{bmatrix}, \\ X_{i \neq 0} &= \begin{bmatrix} 1 & -\frac{1 + \sin \eta}{\cos \eta} \\ -\frac{1 + \sin \eta}{\cos \eta} & \left(\frac{1 + \sin \eta}{\cos \eta}\right)^2 \end{bmatrix}. \end{aligned}$$

Amazingly, for all $i \neq 0$ the matrices X_i are identical in each order of ζ^i for large k . Now, F in Eq. (21) annihilates all such X_i , i.e., $X_{i \neq 0}F \equiv 0$. Thus, the combination $[\mathbb{I} - 2G(z)D]^{-1}F(z)$ in Eq. (22) results in a single term,

$$\bar{\psi}_0 \sim \frac{1}{2\zeta} \begin{bmatrix} -1 - \sin \eta & -\cos \eta \\ \frac{1 + \sin \eta}{\cos \eta} & 1 + \sin \eta \end{bmatrix} \frac{\psi_{IC}}{\sqrt{N}}, \quad (34)$$

near $z = 1$, entirely independent of k . Hence, it remains $|\psi_{0,t}^2| \sim \frac{1}{N}$ for all times. We show simulations for $|\psi_{0,t}^2|$ with $D = \mathbb{I}$ for various sizes N in Fig. 6.

D. Discussion of Non-Reflective Search Operators

In a further exploration of universality classes for quantum search, we want to investigate the effect of more general search operators. Tulsi [70] has shown that a search operator \mathcal{R}_w which is non-reflective should not affect the complexity of quantum search significantly. However, that discussion assumed that the network was complete.

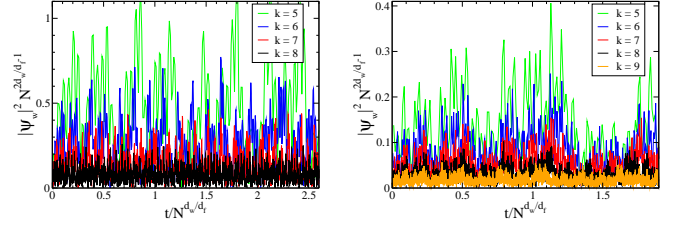


Figure 6. Plot of the probability $p = |\psi_{w,t}^2|$ to detect the quantum walk at site $w = 0$ as a function of time t for DSG of size $N_k = 3^k$ with defective search operators, $D = \mathbb{I}$ (top) and D non-reflective (bottom). Although we have plotted the simulation data on the same scale as in Fig. 5, it is apparent that no effective search is achieved, as predicted by the RG in Eq. (34) and Eq. (37), respectively. There are no discernible peaks, and the probability p to find anything is decaying despite the indicated rescaling with size. Instead, we find $p \sim \frac{1}{N}$ throughout, equivalent to a classical random search for both cases.

As a simple test whether the reflectivity condition on \mathcal{R}_w can be relaxed, we generalize Eq. (17) to

$$D(\phi, \gamma) = e^{i\phi} \cos \phi D(\gamma), \quad (35)$$

which satisfies Eq. (16) but is not hermitian, so $D^2 \neq D$ for all $\phi \neq 0$. For such a case, we find that the RG-analysis produces a very different result that dramatically changes in the limit $\phi \rightarrow 0$.

With the matrix $D(\phi, \gamma)$, the combination $\mathbb{I} - 2G(z)D$ in Eq. (22) is also singular at order ζ^{-1} , and its inverse in Eq. (22) has a similarly leading contribution of order ζ^0 . However, the key cancellation that brought λ_2 to prominence in the ζ^1 -term of $G(z)$ in Eq. (24) is undone in this inversion, due to the non-reflectivity of D : At each order in ζ^j , the most divergent term in k is always $\sim [(1 - e^{i\phi} \cos \phi) \lambda_1^k]^j$, making λ_2 irrelevant unless $\phi = 0$. This property continuous also for $[\mathbb{I} - 2G(z)D]^{-1}F(z)$ in Eq. (22), but incurring an overall factor of λ_1^k as $F(z)$ again annihilates the leading term while providing a factor of ζ^{-1} . Leaving constants of unit-order aside, we then have from Eq. (22):

$$\begin{aligned} \bar{\psi}_0 &\sim \lambda_1^k \left\{ \sum_{j=0}^{\infty} [(1 - e^{i\phi} \cos \phi) \lambda_1^k \zeta]^j \right\} \frac{\psi_{IC}}{\sqrt{N}}, \\ &\sim \frac{N}{1 - (1 - e^{i\phi} \cos \phi) N(z-1)} \frac{\psi_{IC}}{\sqrt{N}}, \end{aligned} \quad (36)$$

since $\lambda_1^k = N$. The inverse Laplace transform then yields

$$\psi_{0,t} \sim \exp \left\{ -\frac{t}{(e^{i\phi} \cos \phi - 1) N} \right\} \frac{\psi_{IC}}{\sqrt{N}}. \quad (37)$$

Ignoring the (rather approximate) complex exponential, which represents a more general function that is bounded for all times t , Eq. (37) again suggest that p will not exceed classical scaling, $\sim \frac{1}{N}$. We show simulations for $|\psi_{0,t}^2|$ with $\phi = \frac{\pi}{4}$ for various sizes N also in Fig. 6, which confirms the RG-prediction.

IV. DISCUSSION

We have indications to believe that the bounds in Eqs. (1-2) are generic for any network characterized in terms of the dimensions d_w^Q and d_f , or d_s , as depicted in Fig. 2. It is straightforward to extend this calculation to other networks, such as the networks MK3 and MK4 discussed in Ref. [46], which lead to identical conclusions aside from minor details in the analysis [47]. A similar RG-analysis has been applied previously to continuous-time quantum search algorithms [59]. Since many quantum computing tasks are similarly defined over a net-

work geometry of interacting variables, we anticipate that our findings would inspire equivalent studies for a broad range of quantum algorithms in the future. For instance, quantum walks also drive the leading quantum algorithm for the element distinctness problem [3], for finding graph isomorphisms [7], as well as for other decision-making processes [71].

Acknowledgements: SB acknowledges financial support from CNPq through the “Ciência sem Fronteiras” program and thanks LNCC for its hospitality. RP acknowledges financial support from Faperj and CNPq.

-
- [1] L. K. Grover, Phys. Rev. Lett. **79**, 325 (1997).
 [2] N. Shenvi, J. Kempe, and K. Whaley, Phys. Rev. A **67**, 052307 (2003).
 [3] A. Ambainis, SIAM J. Comput. **37**, 210 (2007).
 [4] A. Ambainis, International Journal of Quantum Information **1**, 507 (2003).
 [5] S. Shiao, R. Joynt, and S. Coppersmith, Quantum Information & Computation **5**, 492 (2005).
 [6] B. L. Douglas and J. B. Wang, Journal of Physics A: Mathematical and Theoretical **41**, 075303 (2008).
 [7] K. Rudinger, J. K. Gamble, E. Bach, M. Friesen, R. Joynt, and S. N. Coppersmith, Journal of Computational and Theoretical Nanoscience **10**, 1653 (2013).
 [8] X. Qiang, T. Loke, A. Montanaro, K. Aungksunsiri, X. Zhou, J. L. O’Brien, J. B. Wang, and J. C. F. Matthews, Nature Communications **7**, 11511 (2016).
 [9] C. Moore and S. Mertens, *The Nature of Computation* (Oxford University Press, Oxford, 2011).
 [10] R. Motwani and P. Raghavan, *Randomized Algorithms* (Cambridge University Press, 1995).
 [11] A. M. Childs, Phys. Rev. Lett. **102**, 180501 (2009).
 [12] N. B. Lovett, S. Cooper, M. Everitt, M. Trevers, and V. Kendon, Physical Review A **81**, 042330+ (2010).
 [13] A. M. Childs, D. Gosset, and Z. Webb, Science **339**, 791 (2013).
 [14] N. Inui, Y. Konishi, and N. Konno, Physical Review A **69**, 052323+ (2004).
 [15] A. Crespi, R. Osellame, R. Ramponi, V. Giovannetti, R. Fazio, L. Sansoni, F. D. Nicola, F. Sciarrino, and P. Mataloni, Nature Photonics **7**, 322 (2013).
 [16] I. Vakulchyk, M. V. Fistul, P. Qin, and S. Flach, Physical Review B **96** (2017).
 [17] Y. Omar, N. Paunkovic, L. Sheridan, and S. Bose, Phys. Rev. A **74**, 042304 (2006).
 [18] I. Carneiro, M. Loo, X. Xu, M. Girerd, V. Kendon, and P. L. Knight, New Journal of Physics **7**, 156+ (2005).
 [19] A. Schreiber, A. Gábris, P. P. Rohde, K. Laiho, M. Štefaňák, V. Potoček, C. Hamilton, I. Jex, and C. Silberhorn, Science **336**, 55 (2012).
 [20] A. Peruzzo, M. Lobino, J. C. F. Matthews, N. Matsuda, A. Politi, K. Poulios, X.-Q. Zhou, Y. Lahini, N. Ismail, K. Wörhoff, Y. Bromberg, Y. Silberberg, M. G. Thompson, and J. L. O’Brien, Science **329**, 1500 (2010).
 [21] A. Schreiber, K. N. Cassemiro, V. Potoček, A. Gábris, I. Jex, and C. Silberhorn, Phys. Rev. Lett. **106**, 180403+ (2011).
 [22] V. V. Ramasesh, E. Flurin, M. Rudner, I. Siddiqi, and N. Y. Yao, Phys. Rev. Lett. **118**, 130501 (2017).
 [23] E. Venegas-Andraca, Quantum Information Processing **11**, 1015 (2012).
 [24] R. Metzler and J. Klafter, J. Phys. A: Math. Gen. **37**, R161 (2004).
 [25] G. H. Weiss, *Aspects and Applications of the Random Walk* (North-Holland, Amsterdam, 1994).
 [26] S. Redner, *A Guide to First-Passage Processes* (Cambridge University Press, Cambridge, 2001).
 [27] H. B. Perets, Y. Lahini, F. Pozzi, M. Sorel, R. Morandotti, and Y. Silberberg, Phys. Rev. Lett. **100**, 170506 (2008).
 [28] L. Sansoni, F. Sciarrino, G. Vallone, P. Mataloni, A. Crespi, R. Ramponi, and R. Osellame, Phys. Rev. Lett. **108**, 010502 (2012).
 [29] C. Figgatt, D. Maslov, K. A. Landsman, N. M. Linke, S. Debnath, and C. Monroe, Nature Communications **8**, 1918 (2017).
 [30] C. Weitenberg, M. Endres, J. F. Sherson, M. Cheneau, P. Schauss, T. Fukuhara, I. Bloch, and S. Kuhr, Nature **471**, 319 (2011).
 [31] K. Eckert, J. Mompart, G. Birkel, and M. Lewenstein, Phys. Rev. A **72**, 012327 (2005).
 [32] B. C. Travaglione and G. J. Milburn, Phys. Rev. A **65**, 032310 (2002).
 [33] G. S. Engel, T. R. Calhoun, E. L. Read, T.-K. Ahn, T. Mancal, Y.-C. Cheng, R. E. Blankenship, and G. R. Fleming, Nature **446**, 782 (2007).
 [34] M. Mohseni, P. Rebentrost, S. Lloyd, and A. Aspuru-Guzik, The Journal of Chemical Physics **129**, 174106 (2008).
 [35] A. Ambainis, SIGACT News **35**, 22 (2004).
 [36] S. Aaronson and A. Ambainis, Theory of Computing **1**, 47 (2005).
 [37] E. Agliari, A. Blumen, and O. Mülken, Phys. Rev. A **82**, 012305 (2010).
 [38] D. Aharonov, in *Annual Reviews of Computational Physics VI* (World Scientific, 1999) pp. 259–346.
 [39] A. Ambainis, R. Portugal, and N. Nahimov, Quantum Information & Computation **15**, 1233 (2015).
 [40] A. Ambainis, J. Kempe, and A. Rivosh, in *Proceedings of the sixteenth annual ACM-SIAM symposium on Discrete algorithms*, SODA ’05 (Society for Industrial and Applied Mathematics, Philadelphia, PA, USA, 2005) pp. 1099–1108.

- [41] S. Chakraborty, L. Novo, A. Ambainis, and Y. Omar, Phys. Rev. Lett. **116**, 100501 (2016).
- [42] A. M. Childs and J. Goldstone, Phys. Rev. A **70**, 022314 (2004).
- [43] I. Foulger, S. Gnutzmann, and G. Tanner, Phys. Rev. Lett. **112**, 070504 (2014).
- [44] C. Godfrin, A. Ferhat, R. Ballou, S. Klyatskaya, M. Ruben, W. Wernsdorfer, and F. Balestro, Physical Review Letters **119** (2017).
- [45] R. K. Pathria, *Statistical Mechanics, 2nd Ed.* (Butterworth-Heinemann, Boston, 1996).
- [46] S. Boettcher, S. Falkner, and R. Portugal, Phys. Rev. A **91**, 052330 (2015).
- [47] S. Boettcher and S. Li, Physical Review A **97**, 012309 (2018).
- [48] R. Portugal, *Quantum Walks and Search Algorithms* (Springer, Berlin, 2013).
- [49] A. M. Childs and J. Goldstone, Phys. Rev. A **70**, 042312 (2004).
- [50] C. Bennett, E. Bernstein, G. Brassard, and U. Vazirani, SIAM Journal on Computing **26**, 1510 (1997).
- [51] S. Havlin and D. Ben-Avraham, Adv. Phys. **36**, 695 (1987).
- [52] L. P. Kadanoff, Nuovo Cimento **44**, 276 (1966).
- [53] K. G. Wilson, Phys. Rev. B **4**, 3174 (1971).
- [54] N. Konno, Quantum Information Processing **1**, 345 (2002).
- [55] S. Boettcher, S. Falkner, and R. Portugal, Journal of Physics: Conference Series **473**, 012018 (2013).
- [56] G. Grimmett, S. Janson, and P. F. Scudo, Physical Review E **69**, 026119+ (2004).
- [57] A. Tulsi, Phys. Rev. A **78**, 012310 (2008).
- [58] S. Alexander and R. Orbach, J. Physique Lett. **43**, 625 (1982).
- [59] S. Li and S. Boettcher, Phys. Rev. A **95**, 032301 (2017).
- [60] M. Szegedy, Proceedings 45th IEEE Symposium on the Foundations of Computer Science, 32 (2004).
- [61] H. Krovi, F. Magniez, M. Ozols, and J. Roland, Algorithmica **74**, 851 (2015).
- [62] F. Thiel, D. A. Kessler, and E. Barkai, Physical Review A **97** (2018), 10.1103/physreva.97.062105.
- [63] S. Boettcher, S. Falkner, and R. Portugal, Phys. Rev. A **90**, 032324 (2014).
- [64] S. Falkner and S. Boettcher, Phys. Rev. A **90**, 012307 (2014).
- [65] S. Boettcher, B. Gonçalves, and J. Azaret, J. Phys. A: Math. Theor. **41**, 335003 (2008).
- [66] S. Boettcher, S. Li, and R. Portugal, J. Phys. A **50**, 125302 (2017).
- [67] A. Patel and K. S. Raghunathan, Phys. Rev. A **86**, 012332 (2012).
- [68] F. d. L. Marquezino, R. Portugal, and S. Boettcher, Phys. Rev. A **87**, 012329 (2013).
- [69] S. Tamegai, S. Watabe, and T. Nikuni, Journal of the Physical Society of Japan **87** (in press, arXiv:1804.06549).
- [70] A. Tulsi, Phys. Rev. A **86**, 042331 (2012).
- [71] E. Farhi and S. Gutmann, Phys. Rev. A **58**, 915 (1998).

APPENDIX

A. Generalized Unitarity Conditions for Quantum Walks on DSG

Here, we establish generalized unitarity conditions on the propagator \mathcal{U} in the Master equation (3) for the DSG network. For the terms of the propagator pertaining to a generic site $x = 0$ in the DSG, see Fig. 7, we find

$$\begin{aligned} \mathcal{U}_0 = & M(|0\rangle\langle 0| + |1\rangle\langle 1| + |2\rangle\langle 2| + |3\rangle\langle 3|) \\ & + A(|0\rangle\langle 2| + |3\rangle\langle 4| + |2\rangle\langle 1| + |1\rangle\langle 0|) \quad (38) \\ & + B(|0\rangle\langle 1| + |3\rangle\langle 5| + |2\rangle\langle 0| + |1\rangle\langle 2|) \\ & + C(|0\rangle\langle 3| + |3\rangle\langle 0| + |2\rangle\langle 7| + |1\rangle\langle 6|), \end{aligned}$$

where sites labeled $x = 1, \dots, 7$ are all at most two hops away from $x = 0$. However, even of those, we merely keep transition operators $|i\rangle\langle j|$ for which (1) $j = 0$ so that $\mathcal{U}_0|0\rangle \neq 0$, or (2) i is at most one hop away from $x = 0$ (here, $i = 0, 1, 2, 3$). These are the *only* terms that can impact the unitarity condition applicable to site $x = 0$, i.e.,

$$\begin{aligned} \mathcal{U}_0^\dagger \mathcal{U}_0 |0\rangle = & \mathcal{U}_0^\dagger (M|0\rangle + A|1\rangle + B|2\rangle + C|3\rangle), \\ = & (A^\dagger A + B^\dagger B + C^\dagger C + M^\dagger M) |0\rangle \\ & + (A^\dagger B + B^\dagger M + M^\dagger A) |1\rangle \quad (39) \\ & + (A^\dagger M + B^\dagger A + M^\dagger B) |2\rangle \\ & + (C^\dagger M + M^\dagger C) |3\rangle + A^\dagger C |4\rangle \\ & + B^\dagger C |5\rangle + C^\dagger A |6\rangle + C^\dagger B |7\rangle. \end{aligned}$$

As $|0\rangle$ is a *generic* site, its unitarity, $\langle x | \mathcal{U}_0^\dagger \mathcal{U}_0 |0\rangle = \delta_{x,0}$, obtained from Eq. (39), then implies $\mathcal{U}_0^\dagger \mathcal{U}_0 = \mathbb{I}$ for *every* site with the constraints finally summarized in Eq. (7).

B. Renormalization Group (RG)

To accomplish the decimation of the sites $\bar{\psi}_{\{3, \dots, 8\}}$, as indicated in Fig. 3, we need to solve the linear system in Eqs. (6) for $\bar{\psi}_{\{0, 1, 2\}}$. (Note that the following procedure

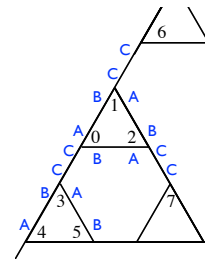


Figure 7. A generic site 0 and seven sites $1, \dots, 7$ that are at most two hops away from 0 on a dual Sierpinski gasket (DSG). Only the relevant hopping operators A, B, C for Eq. (38) are labeled here.

is equivalent to that in Ref. [63], but significantly simplified by the assumption of symmetry, $A = B$, among the hopping operators.) Thus, we expect that $\bar{\psi}_{\{3,\dots,8\}}$ can be expressed as (appropriately symmetrized) linear combinations

$$\begin{aligned}\bar{\psi}_{\{3,4\}} &= P_0\bar{\psi}_0 + Q\bar{\psi}_{\{1,2\}} + R\bar{\psi}_{\{2,1\}} + J\psi_{IC}, \\ \bar{\psi}_{\{5,8\}} &= R_0\bar{\psi}_0 + P\bar{\psi}_{\{1,2\}} + Q\bar{\psi}_{\{2,1\}} + J\psi_{IC}, \\ \bar{\psi}_{\{6,7\}} &= Q_0\bar{\psi}_0 + P\bar{\psi}_{\{1,2\}} + R\bar{\psi}_{\{2,1\}} + J\psi_{IC}.\end{aligned}\quad (40)$$

Inserting this Ansatz into Eqs. (6) and comparing coefficients provides consistently for the unknown matrices $\{P, Q, R, J\}$:

$$\begin{aligned}P &= (M + A)P + A + CR, \\ Q &= (M + C)Q + AR, \\ R &= MR + AQ + CP, \\ J &= I + (M + A + C)J.\end{aligned}\quad (41)$$

Abbreviating $S = (\mathbb{I} - M - C)^{-1}A$ and $T = (\mathbb{I} - M - AS)^{-1}C$, Eqs. (41) have the solution:

$$\begin{aligned}P &= (\mathbb{I} - M - A - CT)^{-1}A, \\ R &= TP, \\ Q &= SR, \\ J &= (\mathbb{I} - M - A - C)^{-1}I.\end{aligned}\quad (42)$$

Finally, after $\bar{\psi}_{\{3,\dots,8\}}$ have been eliminated, we find

$$\begin{aligned}\bar{\psi}_0 &= ([M_0 + 2AP_0] + C_0)\bar{\psi}_0 + A(Q + R)(\bar{\psi}_1 + \bar{\psi}_2) \\ &\quad + (I + 2AJ)\psi_{IC},\end{aligned}\quad (43)$$

and similar for $\bar{\psi}_{\{1,2\}}$. By comparing coefficients between the renormalized expression in Eq. (43) and the corresponding, *self-similar* expression in the first line of Eqs. (6), we can identify the RG-recursions

$$\begin{aligned}M_{k+1} &= M_k + 2A_kP_k, \\ A_{k+1} &= A_k(Q_k + R_k), \\ C_{k+1} &= C_k, \\ I_{k+1} &= I_k + 2A_kJ_k,\end{aligned}\quad (44)$$

where the subscripts refer to k -renormalized (or, unrenormalized) and $(k+1)$ -renormalized form of the hopping operators. These recursions evolve from the unrenormalized ($k=0$) hopping operators with

$$\begin{aligned}\{M, A, C\}_{k=0} &= z\{M, A, C\}, \\ I_{k=0} &= \mathbb{I} \text{ or } 0.\end{aligned}\quad (45)$$

Note that the RG-recursion for $\{M, A, C\}$, the ‘‘engine’’ that drives the walk dynamics, evolves *irrespective* of the specific problem under consideration and independently from I_k . Only $I_{k=0}$ refers to the specific problem one may intend to study, as we discuss in Sec. II. Implementing these recursions in MATHEMATICA, for example, allows a convenient and detailed reproduction of the results presented in the main text.

C. Analysis considering many poles

Here, we present a more elaborate analysis of the Laplace-poles leading to the main result in Eq. (30). Instead of only incorporating the poles closest to the real- z axis, as in Eq. (27), we extend the discussion to allow for a diverging number of such poles, as Fig. 4 would suggest. Such a consideration is well-advised and has proven necessary for some observables [47], although it will only serve to justify our approach in the main text for the present case.

Again, for $t > 0$, $\psi_{0,t}$ should be a periodic function of some fundamental period $T(N) = 2\pi/\theta_k$, but now we want to consider it as a generalized Fourier sin-series, to wit

$$\psi_{0,t} \sim N^\epsilon \left[\sum_{j=1}^{h(N)} f_j \sin(g_j j \theta_k t) \right] \frac{\psi_{IC}}{\sqrt{N}}. \quad (46)$$

To see why this form is justified, we take the Laplace transform as in Eq. (4) to find

$$\begin{aligned}\bar{\psi}_0(z) &\sim N^\epsilon \left[\sum_{j=1}^{h(N)} \frac{f_j}{2i} \left(\frac{1}{1 - ze^{ig_j j \theta_k}} - \frac{1}{1 - ze^{-ig_j j \theta_k}} \right) \right] \frac{\psi_{IC}}{\sqrt{N}}, \\ &\sim N^\epsilon \left[\frac{S_1}{\theta_k} \zeta^0 - \frac{S_3}{\theta_k^3} \zeta^2 + \frac{S_3}{\theta_k^3} \zeta^3 + \frac{S_5}{\theta_k^5} \zeta^4 + \dots \right] \frac{\psi_{IC}}{\sqrt{N}},\end{aligned}\quad (47)$$

where we defined

$$S_m = \sum_{j=1}^{h(N)} \frac{f_j}{g_j^m j^m}. \quad (48)$$

The first line of Eq. (47) reflects the observation, shown in Fig. 4, that $\bar{\psi}_0(z)$ possesses a set of Laplace-poles on the unit-circle in the complex- z plane, symmetric around the real- z axis, that increasingly impinge on that real axis at $z = 1$. Near there, these poles are roughly equally spaced, as expressed by multiples of a phase-angle, $j\theta_k$, where g_j represents some almost-constant function of j that captures any irregularities in the spacings. The function $h(N)$ allows for the possibility that a diverging number of such poles could contribute [47]. In turn, the residues at those poles, $N^\epsilon f_j$, are the amplitudes for each mode in Eq. (46). As $|\psi_{0,t}|$ is bounded, so is $|f_j| N^{\epsilon-1/2}$ both as a function of index j and N . Accordingly, there must be some m_0 such that the sums in Eq. (48) are convergent for $m \geq m_0$, i.e., $S_{m \geq m_0} = O(1)$, independent of $h(N)$. In fact, the boundedness of f_j with j implies that $S_{m \geq 2} = O(1)$. We find that the only consistent choice to match the RG-results in Eq. (26) is to assume that also S_1 is constant, hence, the number of poles that needs to be considered, $h(N)$, does not impact the considerations. Then, we match Eqs. (26) and (47) term-by-term in ζ to get

$$N^\epsilon \frac{S_1}{\theta_k} \sim \lambda_1^k, \quad N^\epsilon \frac{S_3}{\theta_k^3} \sim \lambda_1^{2k} \lambda_2^k, \quad (49)$$

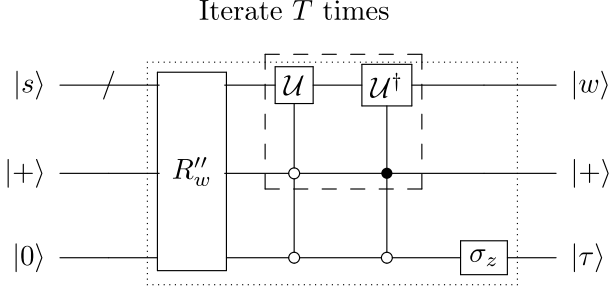


Figure 8. Diagram for the two-qubit extension of the spatial Grover search in Tusli's method. The inner (dashed) box describes the action of the first qubit H'_2 on the original walk-operator \mathcal{U} that yields \mathcal{U}' . It is only the second qubit H''_2 that inserts the tunable parameter τ , whose optimized choice allows to evolve the state of the system from its uniform initial state $|s\rangle$ to overlap with probability $p \sim 1$ with the sought-after state $|w\rangle$ after T iterations, as determined in Eq. (30), of the search propagator $\mathcal{U}''_w = \mathcal{U}'' \mathcal{R}''_w$ (indicated by the faint outer box).

which provides for the characteristic period and the amplitude factor already shown in Eq. (30).

D. Optimized search with Tusli's method

Refs. [57, 70] outline an implementation of the spatial Grover search algorithm for finite-dimensional networks that can dramatically improve the probability to locate the sought-after site w at the optimal time for a measurement. While Tusli introduces the idea first to obtain the most efficient search algorithm to date on a square lattice [57], we follow here his generalization for arbitrary unitary evolution operators [70], such as \mathcal{U} in Sec. III. Without further assumptions on \mathcal{U} , we then require two extra qubits, as shown in the diagram in Fig. 8. The Hilbert space then becomes $\mathcal{H}'' = H_N \otimes H_C \otimes H'_2 \otimes H''_2$, where $\mathcal{H} = H_N \otimes H_C$ is the original Hilbert space consisting of the real-space H_N and the site-internal coin-space H_C . For example, the walk-operator \mathcal{U} and the search-operator $\mathcal{R}_w = \mathbb{I}_N \otimes \mathbb{I}_C - |w\rangle\langle w| \otimes (2D)$, and the unitary “search”-propagator $\mathcal{U}_w = \mathcal{U} \cdot \mathcal{R}_w$, as discussed in Sec. III, are operators in \mathcal{H} . Then, let H_2 be a qubit 2-state space, in which we conveniently define the projectors $\mathbb{P}_s = |s\rangle\langle s|$, with $s \in \{0, 1\}$ for each internal state of H_2 . Note that $\mathbb{P}_0 + \mathbb{P}_1 = \mathbb{I}_2$ and $\mathbb{P}_0 - \mathbb{P}_1 = \sigma_z$, where σ_z is a Pauli-matrix.

The first extension of the walk-operator with qubit H'_2 entails (see diagram in Fig. 8):

$$\begin{aligned} \mathcal{U}' &= (c'_1 \mathcal{U}^\dagger) (c'_0 \mathcal{U}), \\ &= (\mathbb{I}_N \otimes \mathbb{I}_C \otimes \mathbb{P}'_0 + \mathcal{U}^\dagger \otimes \mathbb{P}'_1) (\mathcal{U} \otimes \mathbb{P}'_0 + \mathbb{I}_N \otimes \mathbb{I}_C \otimes \mathbb{P}'_1), \\ &= \mathcal{U} \otimes \mathbb{P}'_0 + \mathcal{U}^\dagger \otimes \mathbb{P}'_1. \end{aligned} \quad (50)$$

Furthermore, for the target, we have

$$|w'\rangle = |w\rangle \otimes |\gamma\rangle \otimes |+\rangle, \quad (51)$$

where in coin-space $|\gamma\rangle$ is such that we get the operator $|\gamma\rangle\langle\gamma| = D(\gamma)$ in Eq. (17), and where $|+\rangle = (|0\rangle + |1\rangle)/\sqrt{2}$. Then, the search-operator $\mathcal{R}'_w = \mathbb{I}_N \otimes \mathbb{I}_C \otimes \mathbb{I}'_2 - 2|w'\rangle\langle w'|$ and the search propagator $\mathcal{U}'_w = \mathcal{U}' \mathcal{R}'_w$ follow accordingly. (Under certain conditions on \mathcal{U} , this first qubit may be redundant [70].)

The second qubit H''_2 finally yields the walk-operator

$$\begin{aligned} \mathcal{U}'' &= (\mathbb{I}_N \otimes \mathbb{I}_C \otimes \mathbb{I}'_2 \otimes \sigma''_z) (c''_0 \mathcal{U}'), \\ &= \mathcal{U}' \otimes \mathbb{P}''_0 - \mathbb{I}_N \otimes \mathbb{I}_C \otimes \mathbb{I}'_2 \otimes \mathbb{P}''_1, \end{aligned} \quad (52)$$

and target

$$|w''\rangle = |w'\rangle \otimes |\tau''\rangle, \quad (53)$$

introducing the free parameter τ via

$$|\tau''\rangle = \sin \tau |0''\rangle + \cos \tau |1''\rangle. \quad (54)$$

Then, we finally obtain the search propagator $\mathcal{U}''_w = \mathcal{U}'' \mathcal{R}''_w$ with the search operator

$$\begin{aligned} \mathcal{R}''_w &= \mathbb{I}_N \otimes \mathbb{I}_C \otimes \mathbb{I}'_2 \otimes \mathbb{I}''_2 - 2|w''\rangle\langle w''|, \\ &= \mathbb{I}_N \otimes \mathbb{I}_C \otimes \mathbb{I}'_2 \otimes \mathbb{I}''_2 \\ &\quad - 2|w\rangle\langle w| \otimes D(\gamma) \otimes D' \left(\frac{\pi}{4} \right) \otimes D''(\pi - \tau), \end{aligned}$$

in an obvious adaptation of the matrix D in Eq. (17).

To follow the procedure outlined in Sec. III, we now merely need to first apply sequentially Eqs. (50) and (52) to each hopping operator $\{M, A, C, I\}$ to obtain $\{M'', A'', C'', I''\}$. While the entire fixed-point analysis of the RG in Sec. II does not change, even in the search analysis in Sec. III, we only modify Eq. (26) to read:

$$\bar{\psi}_0 \sim \cot \tau \left\{ (\mathcal{A}\lambda_1^k) F''_0 \zeta^0 + (\mathcal{A}\lambda_1^k)^2 (\mathcal{B}\lambda_2^k) F''_2 \zeta^2 \right\} \frac{\psi_{IC}}{\sqrt{N}}, \quad (55)$$

where the F''_i are now the two-qubit enlarged versions of those matrices in Eq. (26). From this relation, again in comparison with Eq. (28), follow the Tusli-improved Eqs. (31) discussed in Sec. III B 1.